

# Herpes-Type Virus of the Frog Renal Adenocarcinoma

## I. Virus Development in Tumor Transplants Maintained at Low Temperature

CHRISTOPHER W. STACKPOLE<sup>1</sup>

*Department of Biology,<sup>2</sup> Tulane University, New Orleans, Louisiana 70118*

Received for publication 25 February 1969

Development of the herpes-type virus of the frog kidney tumor was investigated by electron microscopy and high-resolution autoradiography in eyechamber transplants of tumor maintained at 7.5 C for up to 27 weeks. Virus particles were first detected at 10 weeks in nuclei containing aggregates of dense granular material. The initial incorporation of a pulse of <sup>3</sup>H-thymidine into these aggregates indicated that they contained newly synthesized viral deoxyribonucleic acid. Capsids enclosing double-shelled cores were labeled with <sup>3</sup>H-thymidine before capsids with dense cores, and intermediate core forms were observed, suggesting that the double-shelled core transforms into the dense core. Particles with dense cores were observed while being enveloped by budding through the inner membrane of the nuclear envelope, and subsequently while being unenveloped in passing through the outer membrane into the cytoplasm. Virus particles within the cytoplasm acquired fibrillar coats and budded into vesicles, from which they were released, in enveloped form, at the cell surface. Tubular forms and particles considerably smaller than virus particles were regularly encountered in infected nuclei, and the relationship of these forms to virus replication is discussed.

The herpes-type virus which replicates in the Lucké renal adenocarcinoma of the frog, *Rana pipiens*, during host hibernation apparently remains cell-associated (23), as do similar viruses of the human Burkitt lymphoma (10) and avian Marek's disease (1, 9). Prolonged maintenance of the frog kidney tumor at low temperature suppresses cellular deoxyribonucleic acid (DNA) synthesis and stimulates virus production (23), enabling the sequence of virus development in the natural host cell to be determined by monitoring viral DNA synthesis directly with <sup>3</sup>H-thymidine. Tumor transplants in frog anterior eyechambers are well-suited for such an analysis, since virus replication was found to be relatively synchronous in isolated transplants and is apparently more controlled than in *in situ* tumors, persisting longer and resulting in less cell lysis. Previous studies of virus maturation (12, 19, 42) have been limited to examination of primary tumors ravaged by uncontrolled infection. It was felt that an investigation of herpes-type virus development in frog tumor cells, under controlled but essentially natural conditions, should precede *in vitro* studies on the nature of cell-virus interactions in this tumor.

<sup>1</sup> Present address: Division of Immunology, Sloan-Kettering Institute for Cancer Research, New York, N.Y. 10021.

<sup>2</sup> Chapman H. Hyams III Laboratory of Tumor Cell Biology.

## MATERIALS AND METHODS

**Animal and tumor source.** Adult *R. pipiens* were supplied by J. M. Hazen & Co., Alburg, Vt. Two frogs maintained at 22 to 25 C for several months developed kidney tumors spontaneously; these tumors were selected for transplantation because of their rapid growth, as determined by palpation, and because virus has not been observed in tumors developing at this temperature (23).

**Tumor transplantation.** Tumor-bearing frogs and hosts for transplants were anesthetized with 0.5% MS-222 (tricaine methanesulphonate; Sandoz Pharmaceuticals, Hanover, N.J.). Healthy peripheral tumor tissue was removed into amphibian Ringer's solution at 4 C, and 1- to 2-mm<sup>3</sup> pieces were implanted into anterior eyechambers of adult frogs; adjacent pieces were prepared for electron microscopy. Host animals were maintained at 7.5 ± 0.5 C without feeding.

**Electron microscopy.** Tissue was fixed in 4% glutaraldehyde in 0.1 M sodium cacodylate buffer, post-fixed in 1% cacodylate-buffered OsO<sub>4</sub>, and embedded in Epon. Thin sections were cut with glass knives on a Porter-Blum MT-2 microtome, stained with uranyl acetate and lead citrate, and examined with an RCA EMU-3F or Siemens Elmiskop IA electron microscope.

**Virus preparations.** Transplants supporting advanced virus infection were frozen and thawed several times and homogenized in distilled water with a Dounce glass homogenizer. Crude homogenates were

applied to carbon-coated grids, negatively stained with 2% phosphotungstic acid (pH 6.5), and examined with a Siemens electron microscope at 80 kv.

**Pulse-labeling.** Transplants were removed from eyechambers and labeled with 5  $\mu$ c of thymidine-methyl- $^3$ H (Schwarz BioResearch, Orangeburg, N.Y.; specific activity, 3.0 c/mole) per ml in Ringer's solution at 7.5 C for 1 hr; portions of each transplant were fixed for electron microscopy immediately, and the remainder was washed in 0.1% unlabeled thymidine at 7.5 C for 3 hr. Transplant tissue to be fixed 4 hr after labeling was retained in Ringer's solution, and other pieces were retransplanted to new eyechambers and maintained at 7.5 C until preparation for electron microscopy 8, 24, 48, and 72 hr after labeling.

**Autoradiography.** Electron microscope autoradiography was performed according to Salpeter and Bachmann (31), with certain modifications (J.-P. Revel and E. Hay, *personal communication*). Thin sections mounted on celloidin-coated glass slides were stained with uranyl acetate and lead citrate, carbon-coated, and covered with a monolayer of diluted Ilford L4 emulsion from which much of the gelatin was removed by centrifugation. Slides were exposed for 8 to 12 weeks at 4 C, developed in Microdol-X at 18 C for 3 min, and fixed in Kodak acid fixer for 1 min. The celloidin films were floated onto water, and grids were applied to the sections, removed, and examined without further staining.

**Enumeration of virus particles.** The total number of each form of virus particle present in infected transplant cell nuclei was estimated by a modification of the method of Séchaud et al. (32). The number of particles in a section through a nucleus was related to the total number of particles in that nucleus by determining the proportion of the total nuclear volume represented by the section and the mean number of successive sections in which a single particle appears. Section thickness and the number of sections per particle were determined from serial sections through several virus-infected nuclei. From estimates of section and nuclear volumes and direct particle counts, the approximate number of particles per nucleus was calculated.

## RESULTS

**Primary sequence of virus development.** Eighty-five transplants from two frog kidney tumors were maintained at low temperature for as long as 27 weeks and were prepared for electron microscopy at weekly intervals. Neither virus particles nor cellular changes typically associated with virus replication were observed in 20 transplants examined during the first 9 weeks. Five transplants prepared at 10 weeks each contained some cells with herpes-type virus particles, as did all 60 transplants studied subsequently. The degree of infection, which increased progressively with increasing time at low temperature, was comparable in all transplants prepared at any one time, indicating that virus production is probably initiated in all transplants at about 10 weeks and proceeds

with relative synchrony. Lysis of infected cells was rarely observed during the following 17 weeks, suggesting that many cells continued to support virus replication throughout this period.

Virus-infected tumor transplant cells were characterized by a swollen nucleus, in which the chromatin is condensed against the nuclear envelope (marginated), the nucleolus is peripherally displaced, and the nuclear matrix consists of finely granular material of low electron density (Fig. 1). Numerous virus particles and small dense granular aggregates were dispersed throughout the nuclear matrix. In the cytoplasm, the Golgi complex was more extensive than in uninfected cells and was generally represented by numerous large vesicles; glycogen was usually present in infected cells in greater amounts than in uninfected cells. There were no apparent differences between mitochondria of infected and uninfected cells.

Incorporation of  $^3$ H-thymidine by tumor transplant cells in a pattern indicative of cellular DNA synthesis decreased gradually after transplantation, reaching a level too low to be detected by autoradiography within 3 weeks. Detectable incorporation was resumed 10 weeks after transplantation and was confined to nuclei containing virus particles. In cells beginning virus production, a 1-hr pulse of  $^3$ H-thymidine was incorporated initially into large nuclear "complexes" of aggregates consisting of dense irregular 20- to 40-nm granules (Fig. 2). During the first week of virus replication, the number of dense granular aggregates increased, and they became dispersed throughout the nuclear matrix as separate foci, 75 to 150 nm in size, rather than remaining consolidated in complexes (Fig. 1). There was no significant change in the number and distribution of dense aggregates thereafter. At all stages of infection, a 1-hr pulse of  $^3$ H-thymidine was initially detected in dense granular aggregates. After 4 hr, the nuclear matrix was labeled more than the dense aggregates (Fig. 3; Table 1). It has not been ascertained whether the initial production of dense granular material precedes virus particle formation.

The first virus particles produced in tumor transplant cells were confined to the nucleus: empty capsids, 100 nm in diameter and 12.5 nm in thickness, and similar capsids enclosing double-shelled cores (Fig. 2, 4, and 5). The outer shell of this core, 67 nm in diameter and 12.5 nm in thickness, in section resembles the surrounding capsid, whereas the inner shell, 42.5 nm in diameter and about 1.5 nm in thickness, stains densely with uranyl acetate. In negatively stained preparations, the capsid consists of hollow capsomers 10 nm in diameter, arranged in an icosahedral pattern. The outer shell of the double-shelled core

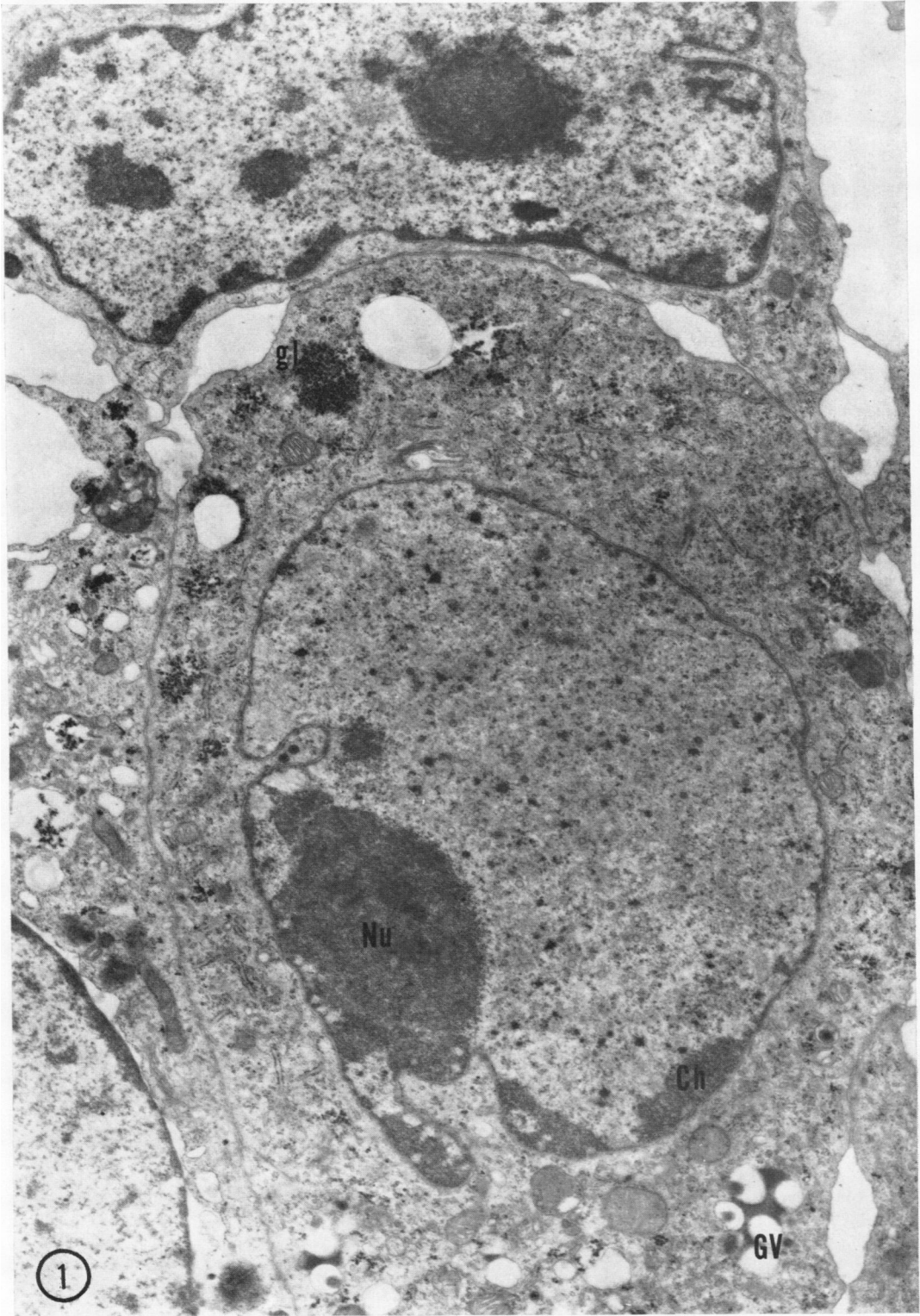


**FIG. 1.** *Virus-infected and uninfected (top) tumor transplant cells. The infected nucleus contains numerous virus particles and dense granular aggregates. Nu, nucleolus; Ch, chromatin; GV, Golgi vesicles; gl, glycogen (20 weeks after transplantation).  $\times 11,000$ .*

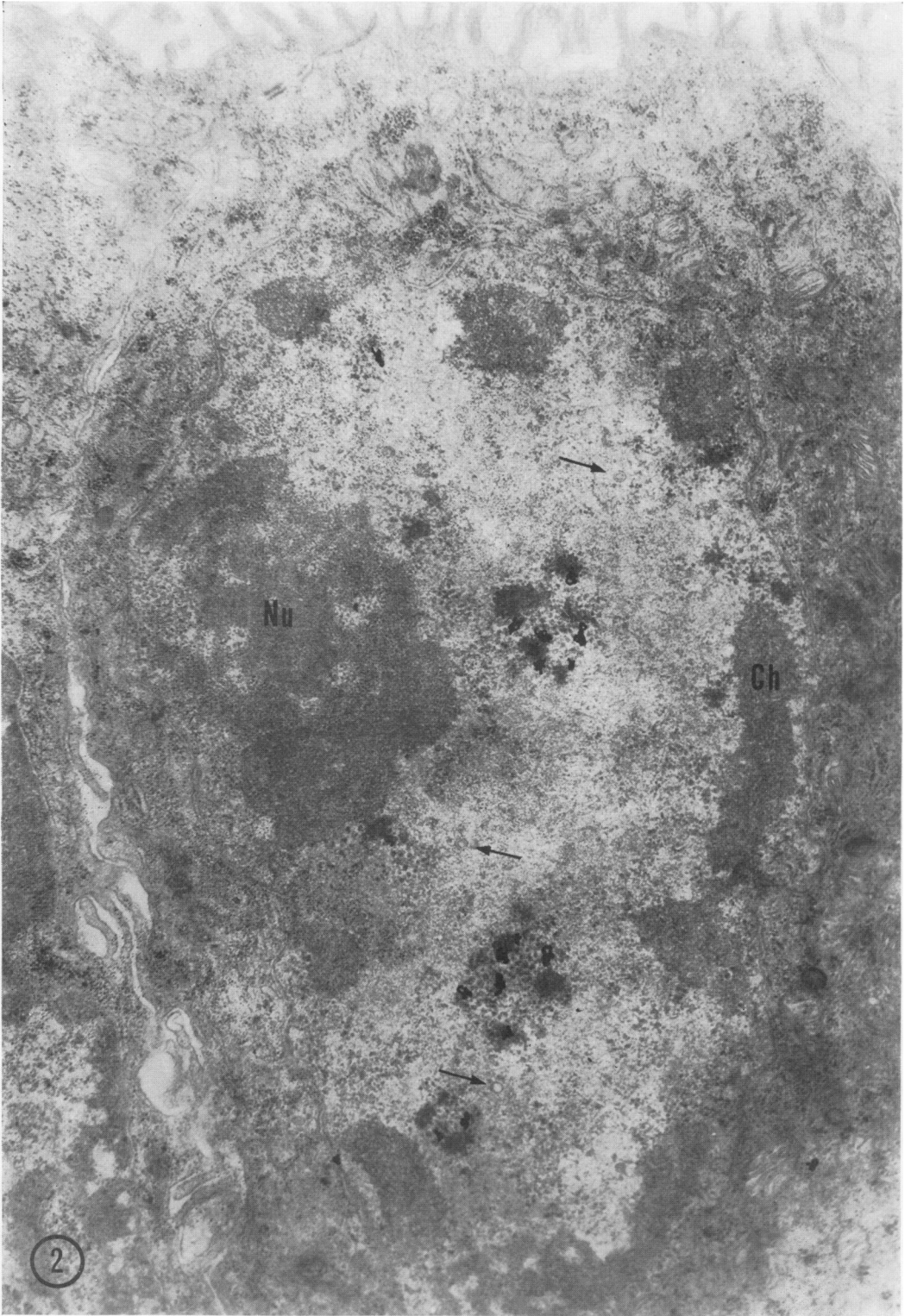


FIG. 2. Autoradiograph of a transplant cell in an early stage of infection. Silver grains are concentrated over "complexes" of dense granular material, immediately after a 1-hr pulse of  $^3\text{H}$ -thymidine. Arrows indicate virus particles. Nu, nucleolus; Ch, chromatin (12 weeks).  $\times 18,000$ .

TABLE 1. Autoradiographic grain distribution in infected transplant cell nuclei after a 1-hr pulse of  $^3\text{H}$ -thymidine<sup>a</sup>

Time after pulse label	Total grain count	Grain distribution (%)				
		Dense granular aggregates	Nuclear matrix	Virus particle types		
				Double-shelled core	Dense core	Nuclear sac
<i>hr</i>						
0	143	91	6	1		
4	225	18	72	6	1	
8	291	2	68	8	17	4
24	384	1	62	11	15	8
48	360	3	72	7	12	5
72	326	2	63	9	16	9

<sup>a</sup> Chased with unlabeled thymidine. Transplants were labeled similarly 12, 20, and 27 weeks after transplantation, and grain counts were compiled from all three series. A virus particle was considered labeled if it was at least partially covered by a silver grain in regions of grain concentration over aggregates of a single particle type.

appears to consist of subunits, whereas the inner shell is impermeable to the stain. Both particle types were initially observed in the nuclear matrix and were not associated with dense granular aggregates, marginated chromatin, or nucleoli. No preliminary stages of assembly or forms intermediate between these two types of particle have been observed. Subsequently, a third type of particle was formed: a 100-nm capsid enclosing a dense core, or nucleoid, typically about 50 nm in diameter and centrally located within the capsid (Fig. 4 and 5). The core of this particle has an electron density comparable to that of the dense granular aggregates, but there was no indication of a direct relationship between virus particles and aggregates. A densely staining demarcation of the inner surface of the capsid was distinctive of this type of particle and may account for the apparent failure of negative stain to penetrate the capsid.

Eight hours after a pulse of  $^3\text{H}$ -thymidine, the nuclear matrix was strongly labeled, with negligible label in the dense aggregates (Table 1). Incorporation of label into virus particles cannot be determined accurately when particles are dispersed throughout the nucleus but can be estimated when silver grains are concentrated over aggregates of a single type of particle. The only virus particles in which significant label could be so detected after 4 hr were capsids enclosing double-shelled cores (Fig. 6). By 8 hr, particles with dense cores were also labeled (Fig. 7). Both of these virus forms, as well as the nuclear matrix,

remained labeled for at least 72 hr, although particles with double-shelled cores were never strongly labeled (Table 1). Most of the label in infected transplants homogenized with 3% sodium dodecyl sulfate 24 hr after a pulse of  $^3\text{H}$ -thymidine was detected in ethyl alcohol-insoluble material, presumably DNA.

Estimation of the total number of each form of virus particle in infected nuclei at various intervals after the initiation of virus production (Fig. 9) indicates that empty capsids increased almost 60-fold during 17 weeks of virus production, the most marked increase occurring within the first 4 to 6 weeks. During the same 17-week period, particles with double-shelled cores and dense cores increased only about eightfold. These three particle forms were never observed outside intact nuclei. Alteration of empty capsids was not observed; however, particles with double-shelled cores may be transformed into particles with dense cores, since particles enclosing cores with both shell and dense components were frequently encountered (Fig. 8).

Virus particles with dense cores were often close to the inner membrane of the nuclear envelope (Fig. 7). Particles of this type were observed budding into the space separating the inner and outer membranes of the nuclear envelope, becoming tightly enveloped by a thickened portion of the inner membrane in the process (Fig. 10). A consistent 10-nm space between capsid surface and investing membrane may result from incorporation of additional material. These particles appeared to be extruded from the nuclear envelope (or continuous cisternae of endoplasmic reticulum) by fusion of the membrane surrounding the particle with the outer membrane of the nuclear envelope, with the consequent release of the particle into the cytoplasm (Fig. 11). That these particles were not entering the nuclear envelope from the cytoplasm is evident from the lack of surface coat material, which is always present on cytoplasmic particles (Fig. 18 and 19) but absent from nuclear particles. Numerous virus particles may be retained within the nuclear envelope before release into the cytoplasm. In advanced infection (6 weeks or more), regions of the inner membrane of the nuclear envelope were often greatly distended into the nuclear matrix, forming prominent sacs filled with virus particles, all with dense cores (Fig. 12). These sacs remained continuous with the space separating the membranes of the nuclear envelope. Virus particles were observed entering and being released from these sacs in the same manner as at sites where the nuclear envelope is not distended; envelopment by a thick (about 8 nm) unit membrane resulted in a total particle diameter of 130

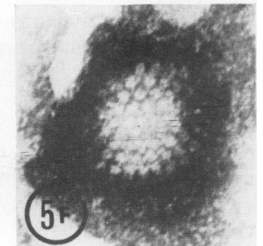
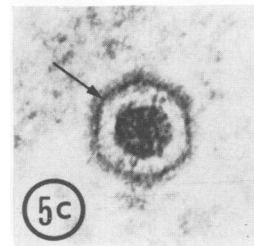
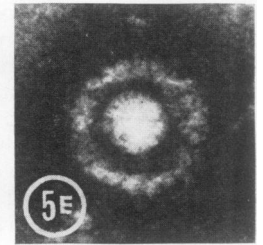
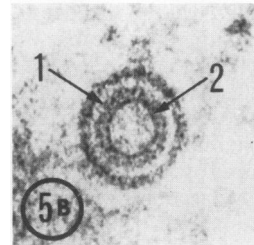
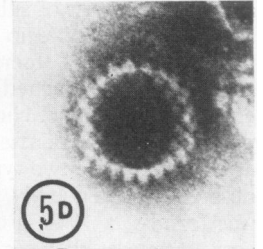
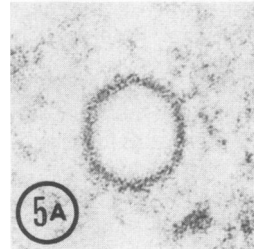
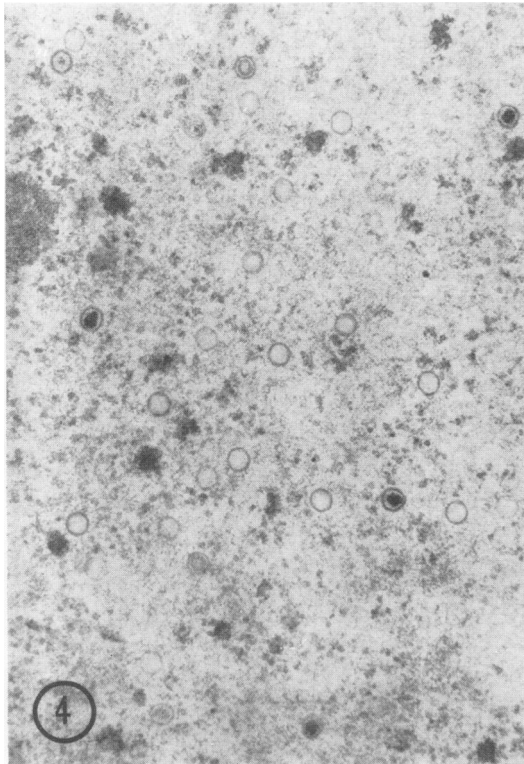
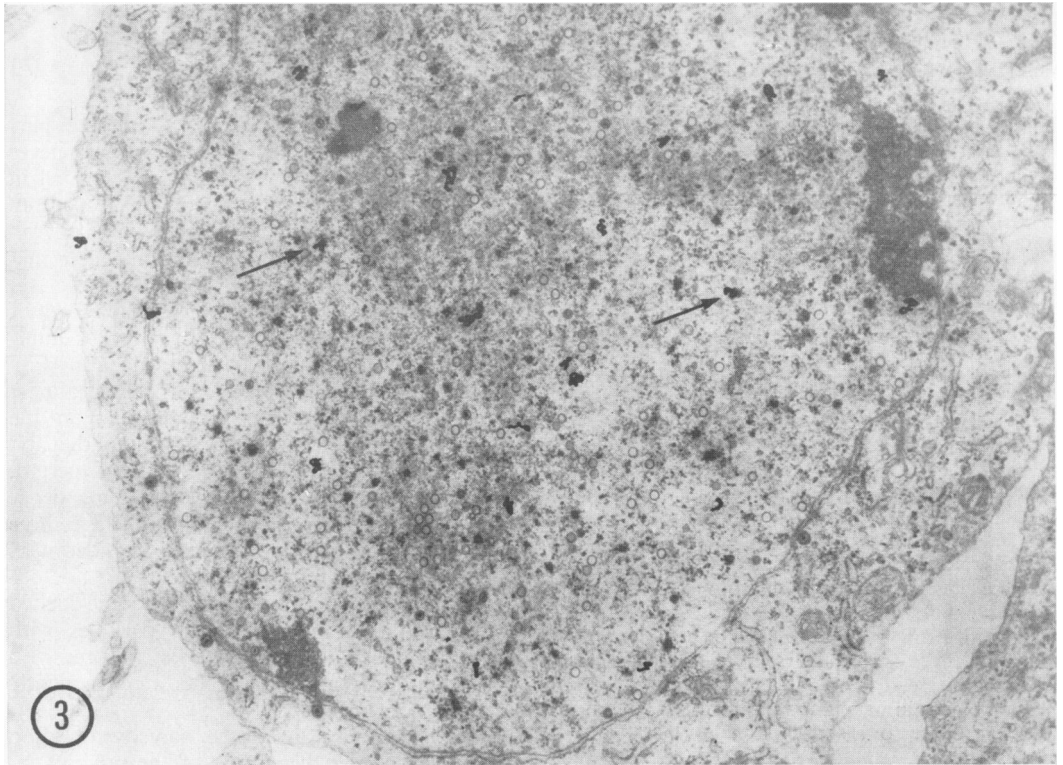


FIG. 3. Autoradiographic grains over nuclear matrix and dense granular aggregates (arrows) 4 hr after a pulse-label (12 weeks).  $\times 11,500$ .

FIG. 4. Nuclear virus particles and dense granular aggregates (12 weeks).  $\times 29,000$ .

FIG. 5. Three types of nuclear particles in section (A to C) and corresponding particles negatively stained (D to F); 1 and 2 (Fig. 5B), outer and inner shells of double-shelled core. Arrow (Fig. 5C) indicates demarcation of capsid inner surface in particle with dense core.  $\times 150,000$ .

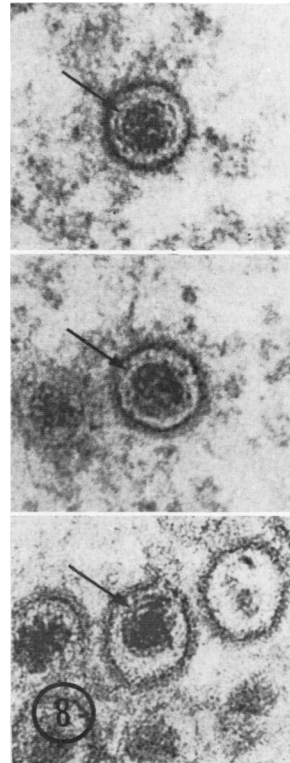
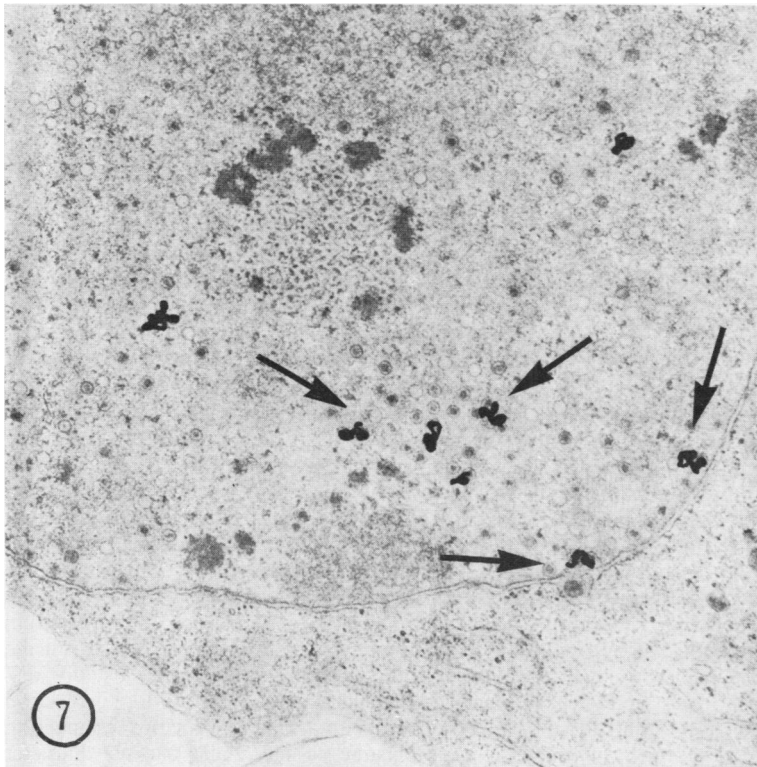
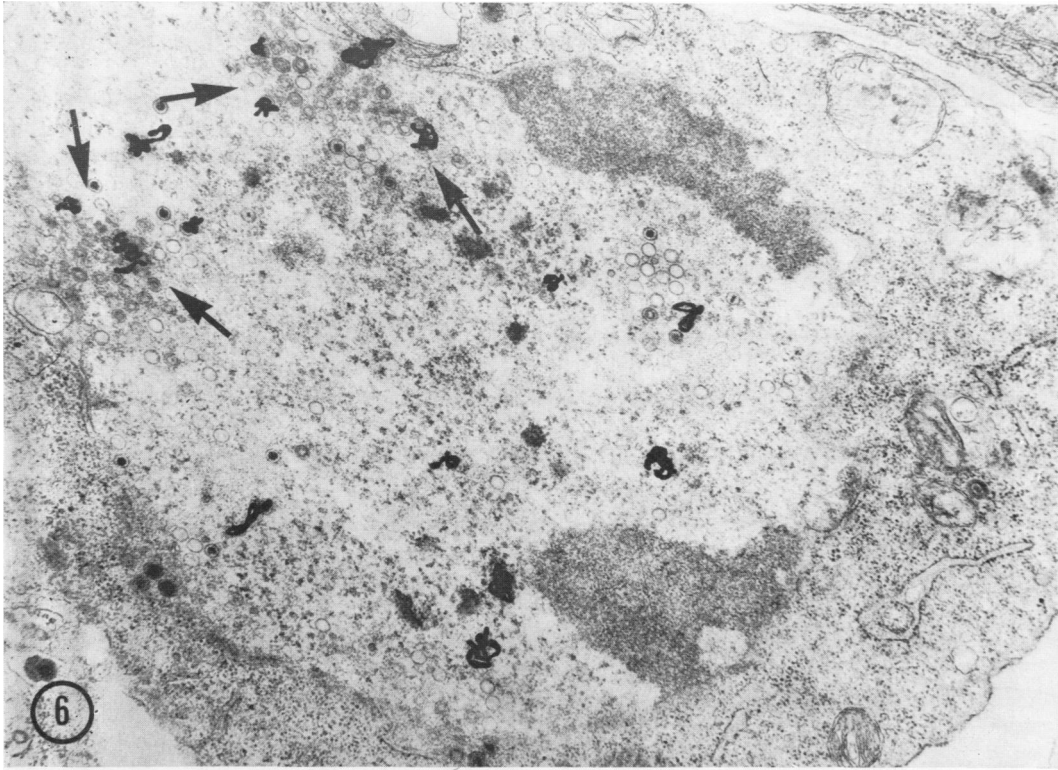


FIG. 6. Autoradiographic grains over aggregates of particles with double-shelled cores (arrows) and over the nuclear matrix, 4 hr after a pulse-label (20 weeks).  $\times 20,000$ .

FIG. 7. Silver grains concentrated over aggregates of particles with dense cores in the nuclear matrix and lining the nuclear envelope (arrows), 8 hr after a pulse-label (20 weeks).  $\times 18,000$ .

FIG. 8. Three nuclear particles with dense cores surrounded by shell-like structures (arrows).  $\times 135,000$ .

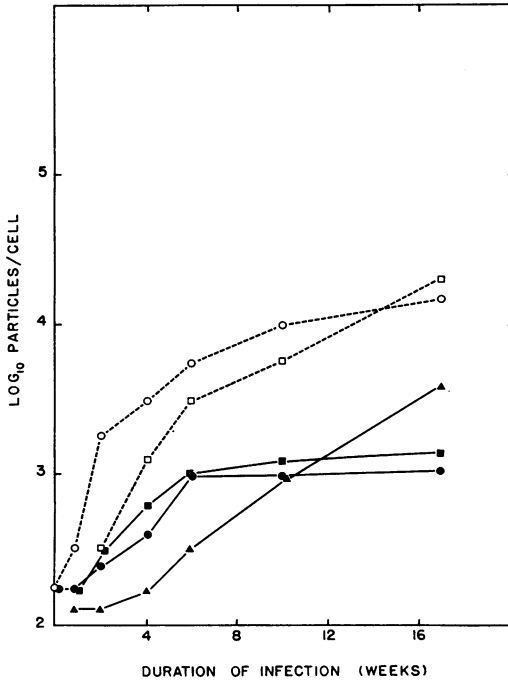


FIG. 9. Approximate numbers of virus particles and viral components in infected tumor transplant nuclei at intervals after the initiation of virus production 10 weeks after transplantation. At each interval, the number of particles in 10 representative sectioned nuclei was counted and the mean number of particles per nucleus was calculated. Counts were made only in cells supporting the most advanced infection and assumed to have initiated virus production 10 weeks after transplantation. Symbols: ○, empty capsids; □, 55-nm particles; ●, capsids with double-shelled cores; ■, capsids with dense cores; ▲, nuclear enveloped particles.

to 135 nm (Fig. 13). The envelope was completely closed and impermeable to negative stain unless it became ruptured (Fig. 14). Entrance into the nuclear envelope was restricted to particles with dense cores. Nuclear sacs of virus were initially labeled with  $^3\text{H}$ -thymidine 8 hr after a 1-hr pulse but were labeled more strongly after 24 to 72 hr (Fig. 15; Table 1). Nuclear enveloped particles increased in number rapidly during advanced infection (Fig. 9), when nuclear sacs containing more than 1,000 particles were not uncommon. The infrequency with which particles were observed entering or being released from the nuclear envelope and nuclear sacs suggests that these processes occur rapidly. Both membranes of the nuclear envelope, but especially the inner membrane, were more extensive and distended in infected cells than in uninfected cells.

Virus particles released into the cytoplasm were initially labeled 24 hr after a pulse-label and were also labeled at 48 and 72 hr (Fig. 16; Table 2). These particles were occasionally observed in the vicinity of sheaths of nearly parallel nonrigid filaments, 25 to 30 nm in diameter and up to 4 to 5  $\mu\text{m}$  in length, composed of finely fibrillar material (Fig. 16 and 17). Cytoplasmic virus particles were always coated with fibrillar material, about 25 nm in thickness, which closely resembles the material comprising the filaments (Fig. 17 and 18). Sheaths of filaments were typically present in the cytoplasm of infected cells, being formed shortly after the initial appearance of virus particles, suggesting a relationship with associated particles. Cytoplasmic virus released from the nuclear envelope always possessed dense cores and was not membrane-invested; fibrils of coat material adhered directly to the capsid, resulting in a total particle diameter of 145 to 150 nm (Fig. 18 and 19). These particles gradually increased in number in infected cells during virus production.

Cytoplasmic virus particles were frequently observed while being enveloped by budding into vesicles in a manner similar to the budding of particles into the nuclear envelope, although complete entrance was never attained (Fig. 20). Most vesicles contained only one particle, although several to many particles were occasionally observed in large vesicles. Cytoplasmic enveloped particles consist of a capsid enclosing a dense core and surrounded by coat material clearly separated from an outer layer of dense granular material, which is closely applied to a thin (about 6 nm) unit membrane continuous with the vesicle membrane; total particle diameter is about 230 nm (Fig. 21). These particles were labeled with  $^3\text{H}$ -thymidine 24 to 72 hr after a pulse-label (Fig. 22; Table 2).

Enveloped virus particles similar to those in cytoplasmic vesicles were often present in extracellular spaces, such as in proximity to the microvilli at the apical surface of infected cells. These particles were released from cytoplasmic vesicles which fused with the cell surface plasmalemma (Fig. 23). Extracellular enveloped virus particles, which were labeled 24 to 72 hr after a pulse-label (Fig. 24), consist of a coated capsid with a dense core, loosely enveloped by a thin unit membrane; granular material of greater electron density than the coat substance is always present between the coat and the investing membrane, usually displaced to one side (Fig. 25). A tail-like projection of the envelope marks the previous connection to a cytoplasmic vesicle. Total particle diameter was 220 to 240 nm.

**Secondary aspects of virus development.** Several virus forms or virus-associated structures reg-

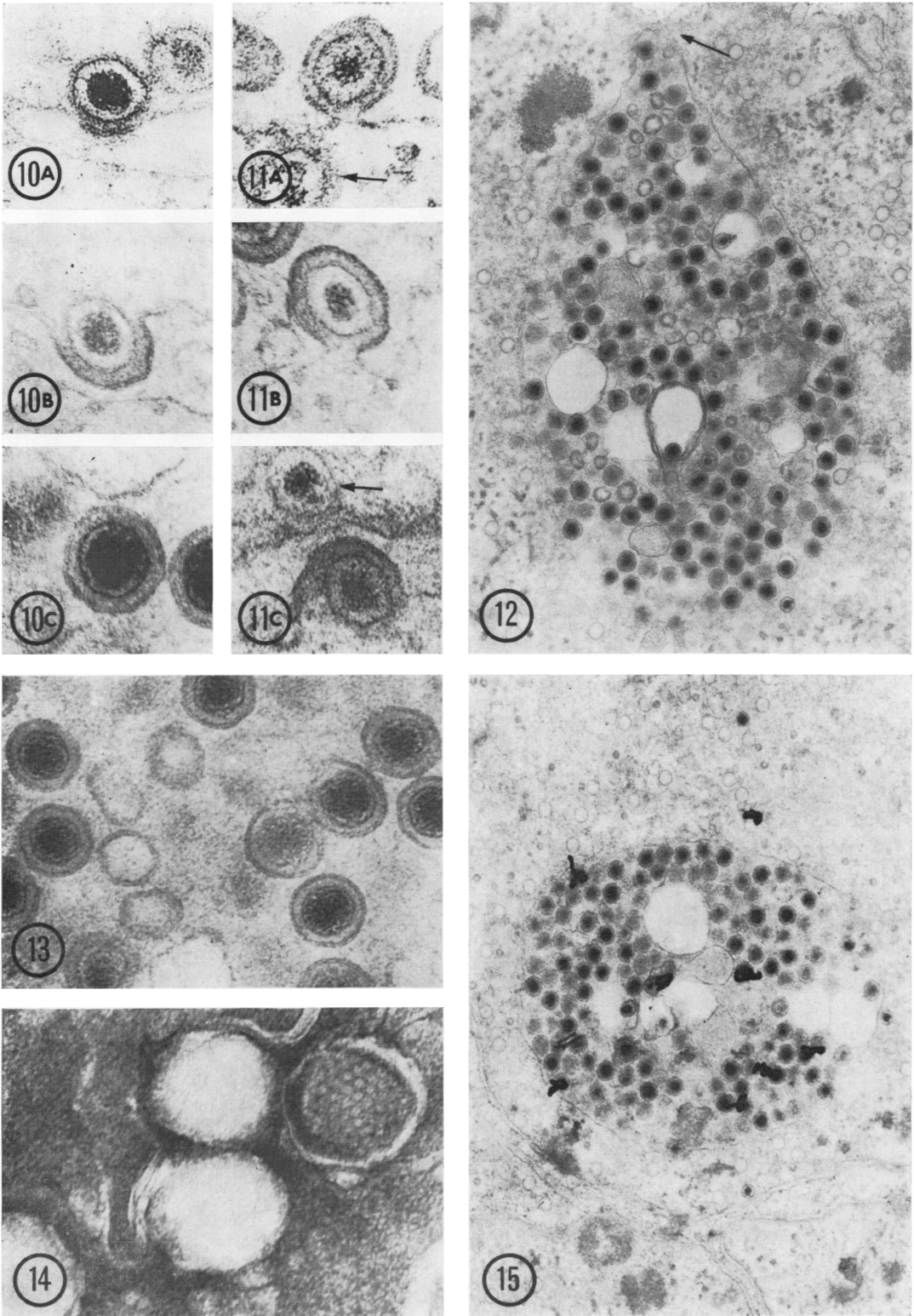


FIG. 10. Sequence (A to C) of virus particle entrance into the nuclear envelope.  $\times 135,000$ .  
 FIG. 11. Sequence (A to C) of particle release from the nuclear envelope into the cytoplasm. Arrows indicate cytoplasmic (A) and nuclear (C) particles.  $\times 135,000$ .  
 FIG. 12. Nuclear sac of virus continuous with the nuclear envelope (arrow); at 27 weeks.  $\times 23,000$ .  
 FIG. 13. Higher magnification of particles in Fig. 12.  $\times 90,000$ .  
 FIG. 14. Negatively stained nuclear sac particles, one ruptured and two impermeable to the stain.  $\times 150,000$ .  
 FIG. 15. Autoradiographic grains over a nuclear sac 24 hr after a pulse-label (27 weeks).  $\times 23,000$ .

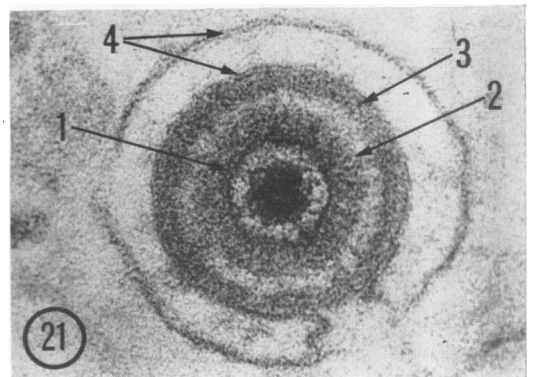
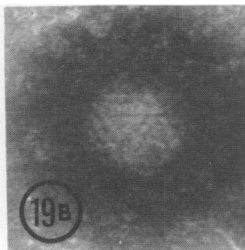
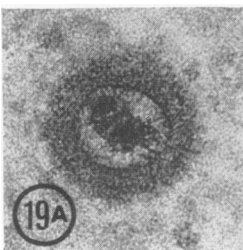
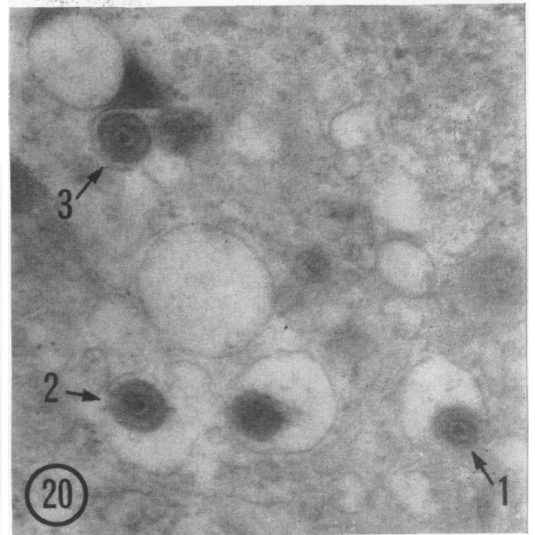
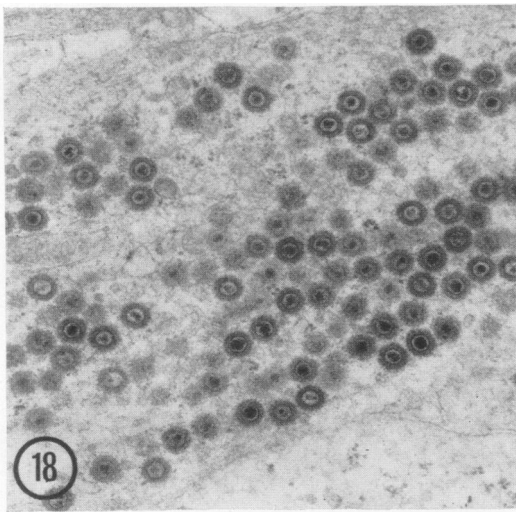
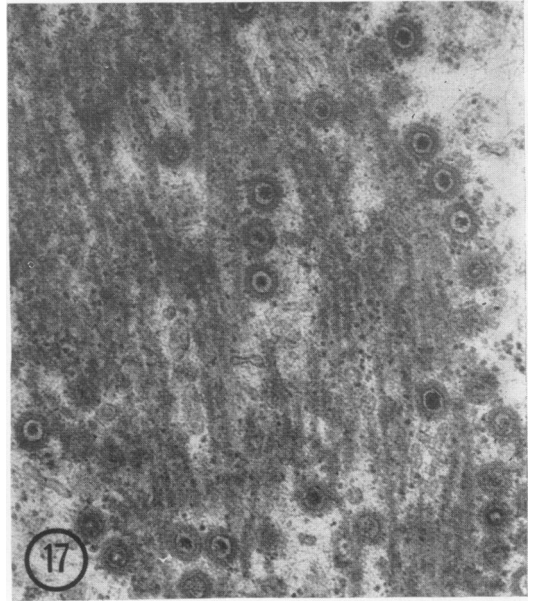
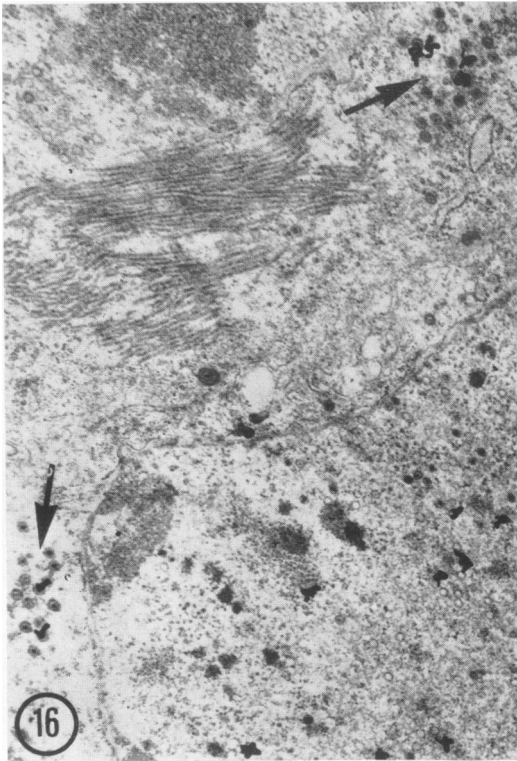


FIG. 16. Autoradiographic grains over cytoplasmic virus (arrows) 48 hr after labeling (27 weeks).  $\times 11,000$ .  
 FIG. 17. Virus particles among cytoplasmic filaments.  $\times 37,000$ .  
 FIG. 18. Cytoplasmic virus particles, all coated and with dense cores (20 weeks).  $\times 28,000$ .  
 FIG. 19. Typical cytoplasmic virus particles, in section (A) and negatively stained (B).  $\times 135,000$ .  
 FIG. 20. Stages (1-3) of virus envelopment by protrusion into cytoplasmic vesicles (16 weeks).  $\times 35,000$ .  
 FIG. 21. Cytoplasmic enveloped virus particle. Symbols: 1, capsid; 2, coat; 3, dense material; 4, envelope continuous with vesicle membrane.  $\times 150,000$ .

TABLE 2. Autoradiographic grain distribution in infected transplant cell cytoplasm and extracellular spaces after a 1-hr pulse of  $^3\text{H}$ -thymidine<sup>a</sup>

Time after pulse label <sup>b</sup>	Total grain count	Grain distribution (%)				
		Cytoplasm	Cytoplasmic virus	Cytoplasmic enveloped virus	Extracellular virus	Extracellular enveloped virus
hr						
24	109	5	57	23	3	12
48	134	3	61	19	5	12
72	158	9	52	15	2	22

<sup>a</sup> Chased with unlabeled thymidine.

<sup>b</sup> At 0 to 8 hr. grain counts were negligible.

ularly encountered during virus production in tumor transplants appeared to be indirectly related to virus maturation.

Nuclear virus particles of the type enclosing double-shelled cores were occasionally incompletely formed, especially during early infection (Fig. 26). In these forms, the capsid was incomplete and the core was complete or incomplete. Other nuclear particles were frequently observed to contain incomplete double-shelled cores (Fig. 27) or atypical dense cores.

In transplants examined 2 weeks after the initiation of virus production, some cells supporting the most advanced stage of infection contained a small number of intranuclear particles smaller than herpes-type virus particles (Fig. 28). These particles consist of an outer shell, 55 nm in diameter and 12.5 nm in thickness, which in section resembles the capsids of associated virus particles, and an inner shell, 28 nm in diameter and about 1.5 nm in thickness, which stains densely with uranyl acetate. When negatively stained, the outer shell appears to consist of subunits, whereas the inner shell is impermeable to the stain. The morphological similarity between this particle and the double-shelled core of associated virus particles (Fig. 5) is striking, despite a size difference. The 55-nm particles were never associated with margined chromatin, nucleoli, or dense aggregates and were not observed outside intact nuclei. They may be distributed throughout the nuclear matrix but were frequently closely associated with aggregates of empty virus capsids (Fig. 29). These particles increased in number almost 50-fold during virus production (Fig. 9). By 17 weeks after the initiation of virus production, 55-nm particles were present in more than 90% of infected cells. Incorporation of  $^3\text{H}$ -thymidine into these particles was not detected, suggesting that they either lack DNA or require more than 72 hr for their formation.

Amid large aggregates of 55-nm particles, tubules 35 nm in diameter and of varying length were often observed (Fig. 30). These tubules were present only in nuclei containing large numbers of 55-nm particles and were frequently continuous with these particles; the surface of negatively stained tubules appeared to be covered with subunits. Tubules of this type were first observed in cells supporting advanced infection 6 weeks after initial virus appearance and were never present in more than 5 to 10% of infected cells at any time. Larger tubules, 65 nm in diameter, were first observed in several infected nuclei 8 weeks after the initiation of virus production (Fig. 31); they were present in only 1 to 5% of infected cells after 17 weeks of virus production and were confined to nuclei containing 55-nm particles and 35-nm tubules. The outer sheath of the 65-nm tubule consists of hollow capsomeres similar to those comprising virus capsids. Tubular forms were not encountered in sufficient numbers to ascertain whether they became labeled with  $^3\text{H}$ -thymidine.

Many cells in advanced infection (6 weeks or more) contained large crystalline arrays of empty virus capsids or 55-nm particles (Fig. 32). Other particle types were not observed to aggregate in such regular patterns.

The nuclear envelope of cells supporting advanced infection was occasionally ruptured, exposing the nuclear contents to the cytoplasm and allowing some nuclear particles to move into the cytoplasm. When this occurred, released particles were covered with a fibrillar coat, 20 to 25 nm in thickness, resembling the coat typically formed around virus particles released into the cytoplasm during virus maturation. Coating of empty capsids and capsids enclosing double-shelled cores often occurred near sheaths of cytoplasmic filaments (Fig. 33). There was a gradation in degree of coating of particles when the nucleus was only partially disrupted, from complete coating within the cytoplasm to a lack of coating in the central nuclear matrix.

In advanced infection, groups of cytoplasmic enveloped virus particles and empty vesicles were occasionally embedded in a dense finely granular material not bounded by a membrane (Fig. 34). This material resembles the layer typically present in enveloped cytoplasmic and extracellular particles between the coated virus particle and the investing membrane. There is also a similarity between this material and the contents of associated lysosome-like bodies.

## DISCUSSION

The initial incorporation of  $^3\text{H}$ -thymidine into dense granular aggregates in virus-infected frog tumor transplant cells and the lack of detectable label in uninfected cells indicate that these aggre-

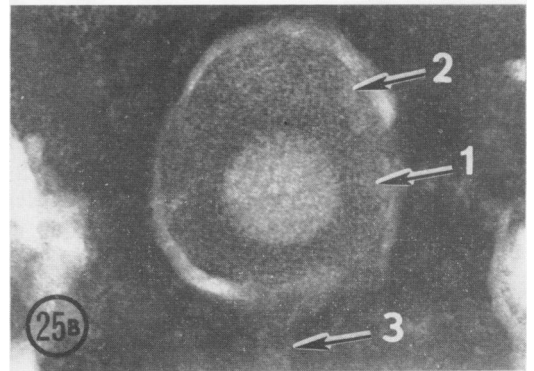
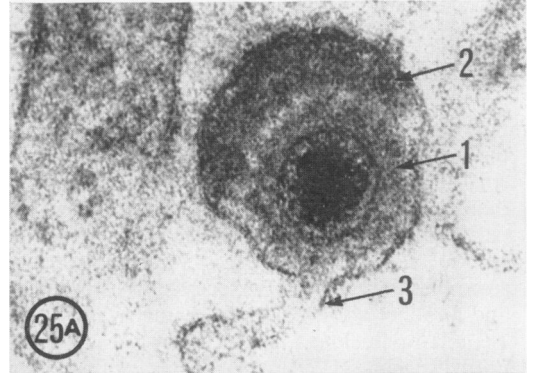
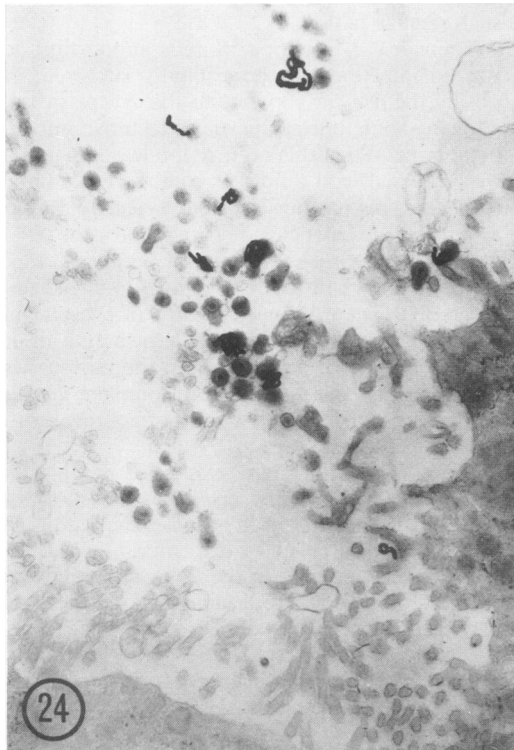
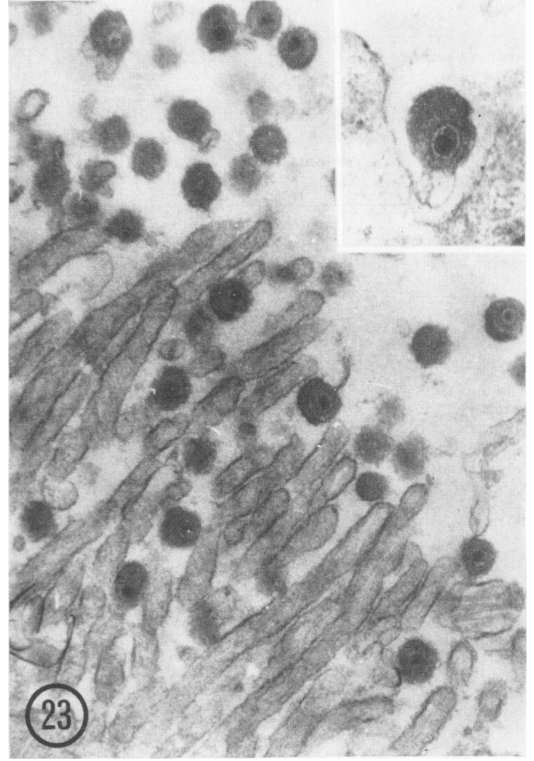
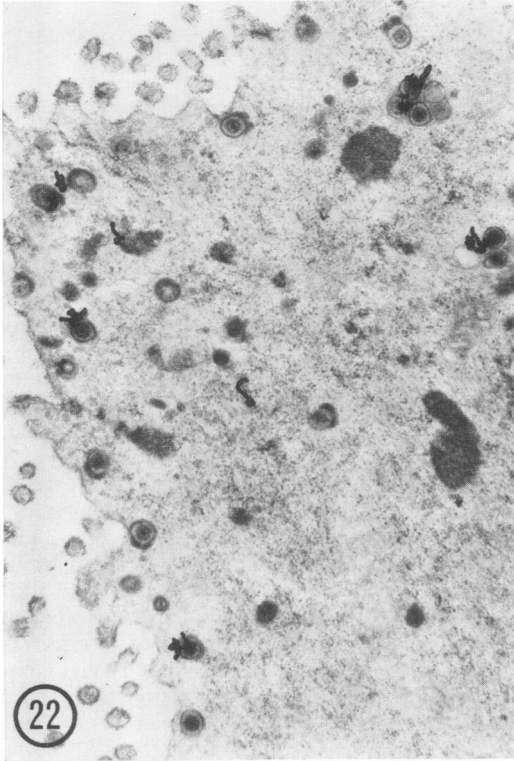


FIG. 22. Autoradiographic grains associated with cytoplasmic enveloped virus 72 hr after a pulse-label (20 weeks).  $\times 13,000$ .

FIG. 23. Extracellular enveloped virus among microvilli at the apical surface of a transplant cell (20 weeks).  $\times 26,000$ . Inset: enveloped particle being released from a vesicle at the surface of an infected cell.  $\times 48,000$ .

FIG. 24. Silver grains over extracellular enveloped virus 48 hr after a pulse-label (27 weeks).  $\times 12,000$ .

FIG. 25. Typical extracellular enveloped virus particles in section (A) and negatively stained (B). Symbols: 1, coat; 2, dense material; 3, "tail" of envelope.  $\times 150,000$ .

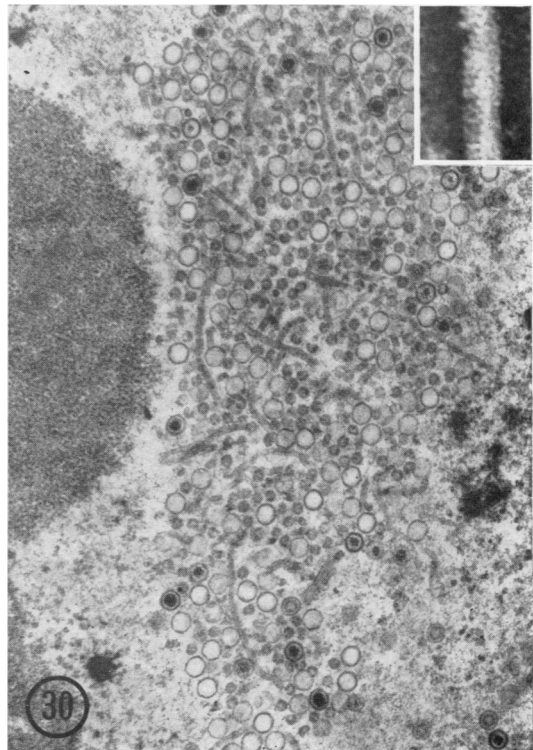
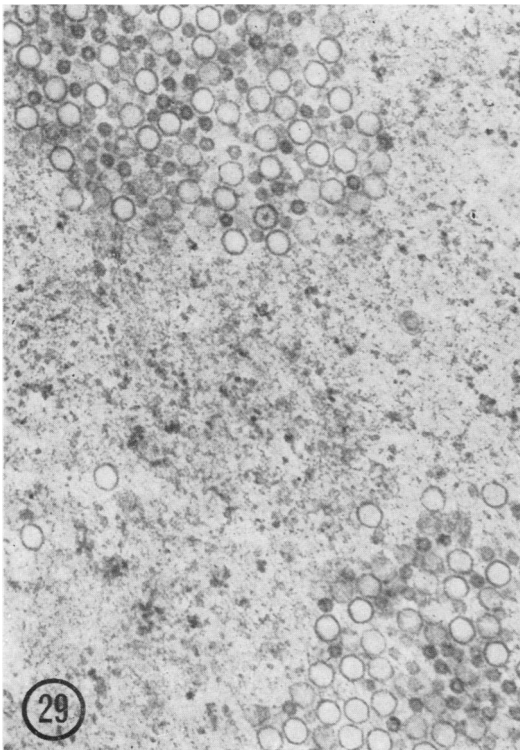
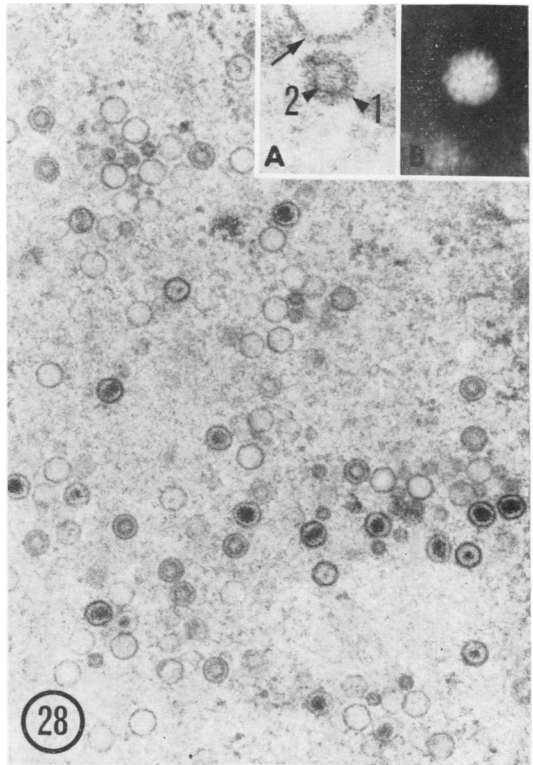
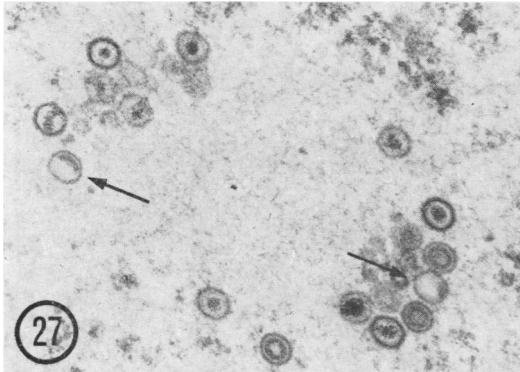
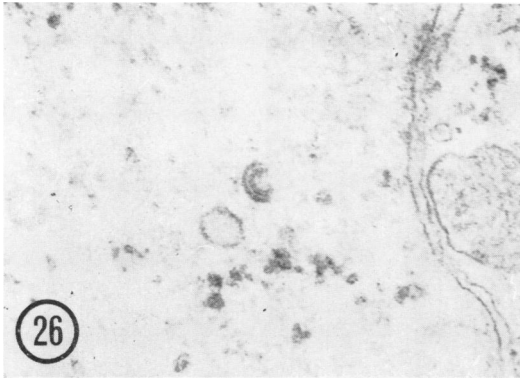


FIG. 26. Virus particle with incomplete core and capsid (11 weeks).  $\times 52,000$ .  
 FIG. 27. Virus particles with incomplete double-shelled cores (arrows) (18 weeks).  $\times 40,000$ .  
 FIG. 28. Nuclear virus and 55-nm particles (12 weeks).  $\times 33,000$ . Insets: 55-nm particles in section (A) and negatively stained (B); 1 and 2, outer and inner shells. Arrow indicates virus capsid.  $\times 150,000$ .  
 FIG. 29. Empty capsids and 55-nm particles aggregated in an infected nucleus (16 weeks).  $\times 32,000$ .  
 FIG. 30. Nuclear aggregate of 55-nm particles and 35-nm tubules (16 weeks).  $\times 28,000$ . Inset: negatively stained 35-nm tubule.  $\times 150,000$ .

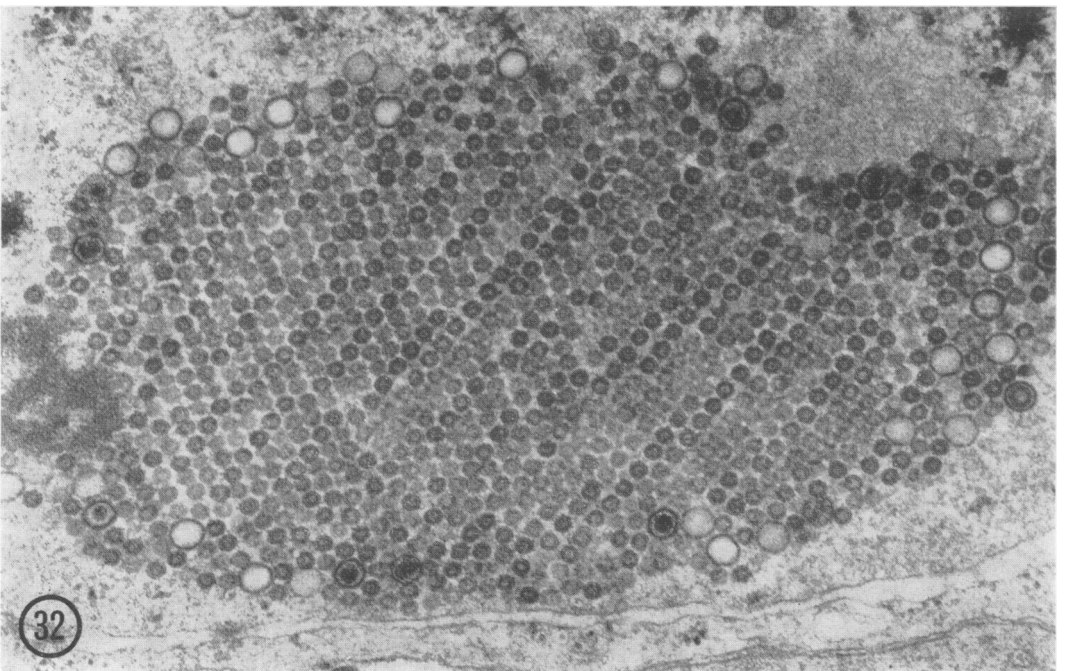
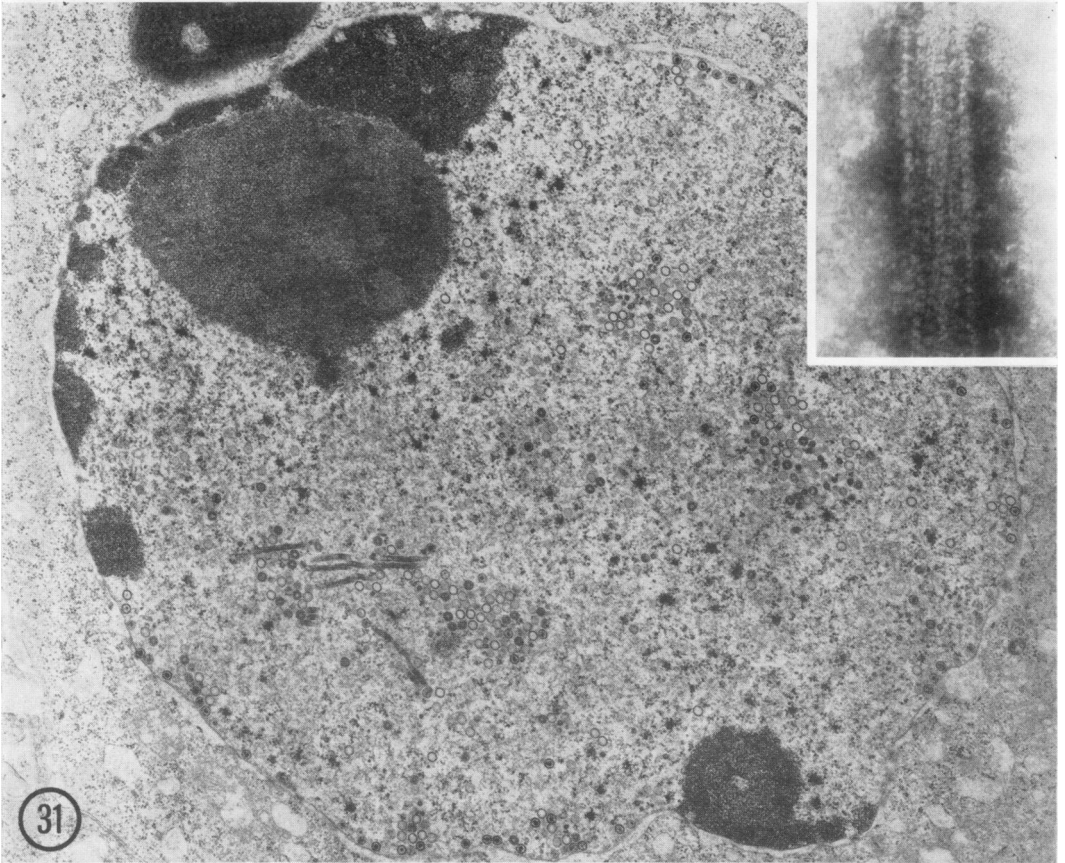


FIG. 31. *Infected transplant nucleus with 65-nm tubules (18 weeks).  $\times 11,000$ . Inset: negatively stained 65-nm tubule.  $\times 150,000$ .*

FIG. 32. *Crystalline array of 55-nm particles in an infected nucleus (20 weeks).  $\times 45,000$ .*

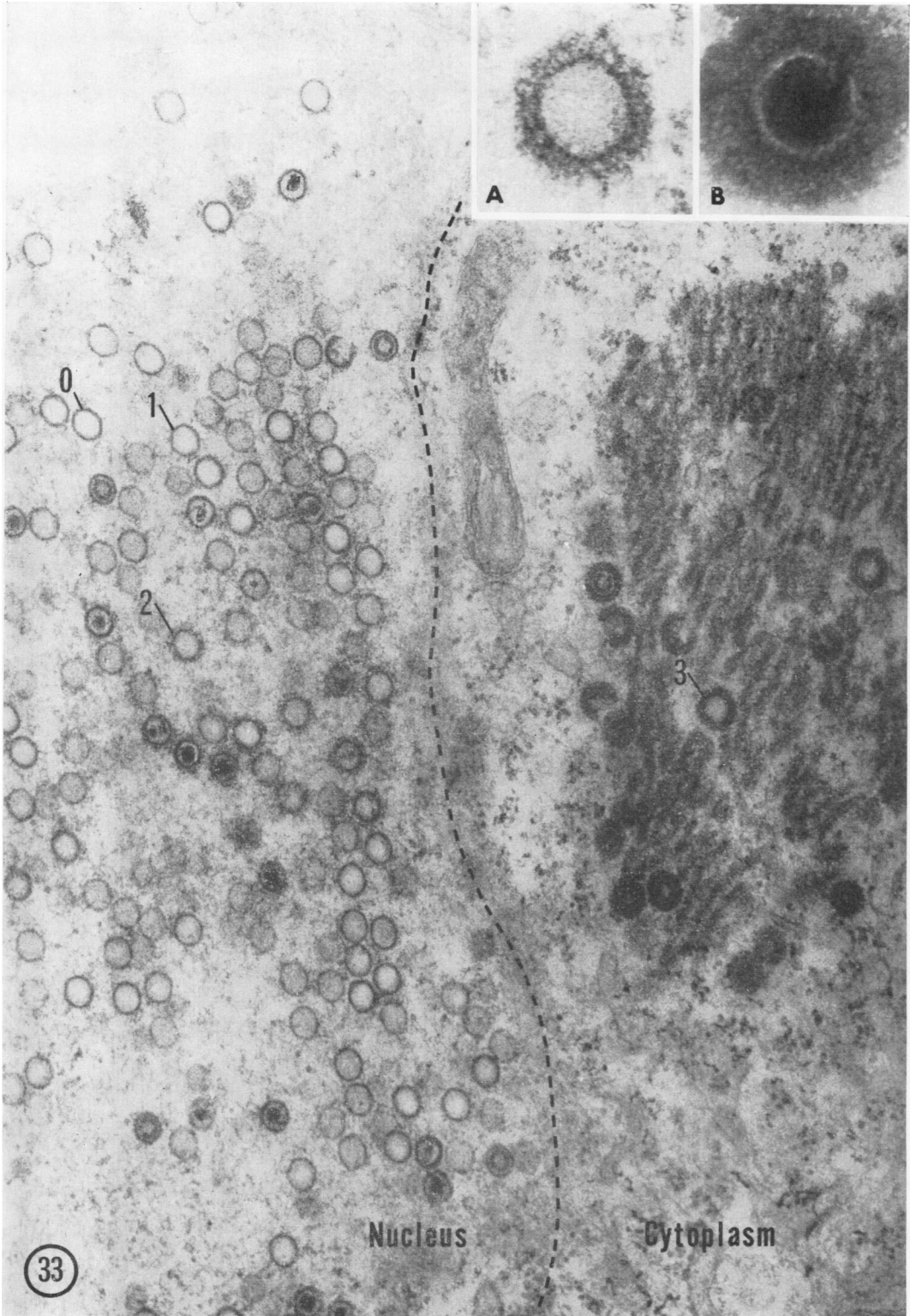


FIG. 33. Portion of a tumor transplant cell supporting advanced infection. The nuclear envelope (former position indicated by dashed line) has ruptured, allowing mixing of nuclear and cytoplasmic contents. Some nuclear particles are associated with cytoplasmic filaments. The degree of virus particle coating (0-3) increases with proximity to the cytoplasm and filaments (27 weeks).  $\times 45,000$ . Insets: coated nuclear particles in section (A) and negatively stained (B).  $\times 150,000$ .

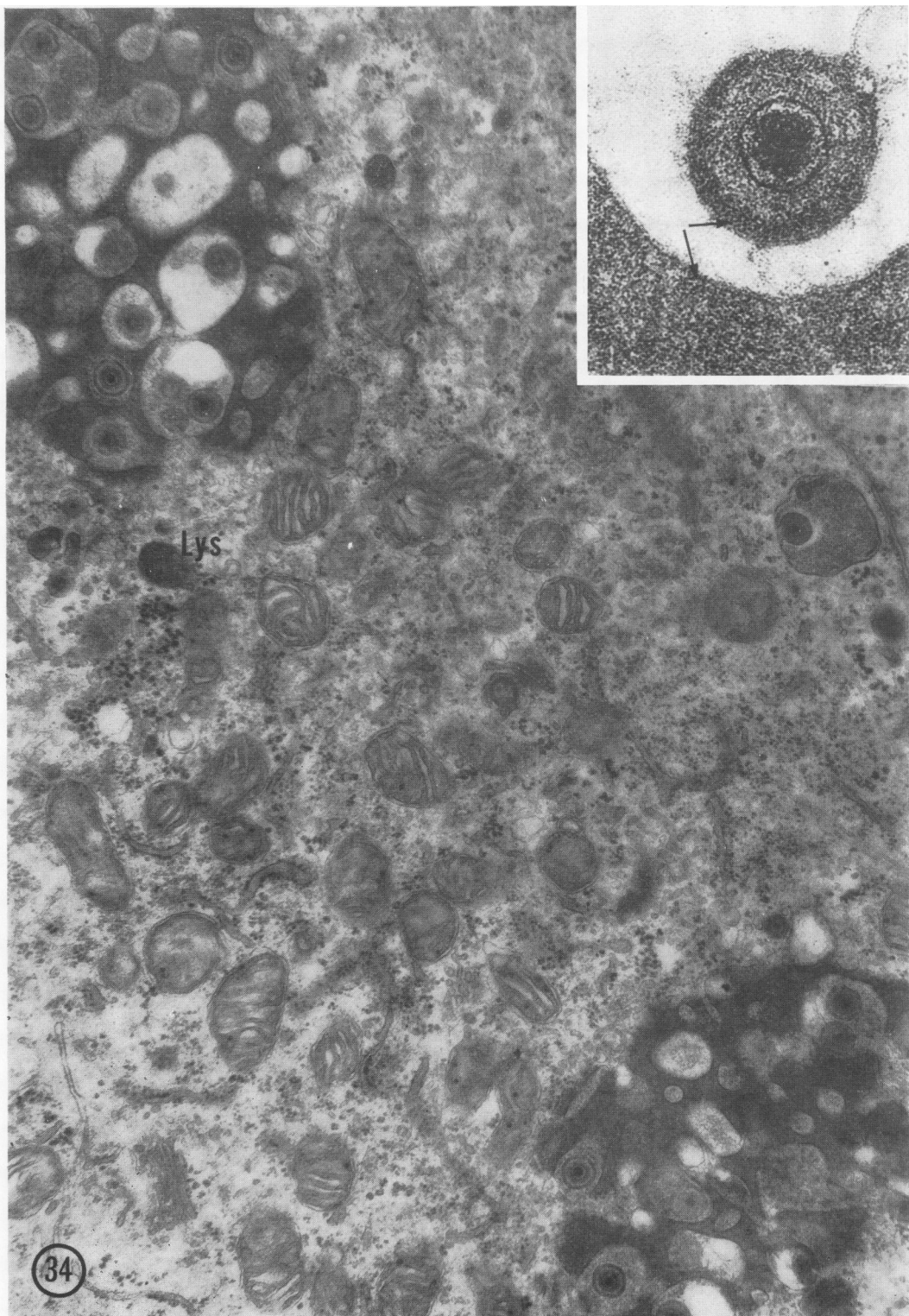


FIG. 34. Cytoplasm of a transplant cell in advanced infection. Two large groups of virus-containing vesicles are embedded in a dense material not bounded by a membrane. The density of this material is similar to the contents of lysozyme-like bodies (*Lys*); at 27 weeks.  $\times 25,000$ . Inset: similarity between inclusion material and dense layer in enveloped virus (arrows).  $\times 150,000$ .

gates consist of, or contain, newly synthesized viral DNA. Dense aggregates have also been observed in nuclei of cells infected with herpes simplex (33, 35, 41), varicella-zoster (39), pseudorabies (13), polyoma (3) viruses and simian virus 40 (14). Since most of the initially incorporated label is detected in the nuclear matrix within 4 hr, viral DNA is presumably synthesized at discrete foci, represented by the dense granular aggregates, and diffuses into the nuclear matrix. Marginated nuclear chromatin and nucleoli are not obviously involved in virus replication, in contrast to a recent report (17).

Empty capsids and capsids enclosing double-shelled cores appear to form spontaneously within the nuclear matrix, since they are not typically associated with any nuclear structures which might serve as templates. Although Morgan et al. (24) suggested that small intranuclear granules may serve as templates for the formation of herpes simplex virus capsids, protein subunits may associate into capsids in the manner of crystal formation, without requiring a template (4). It has been suggested by Fawcett (12) and by Lunger et al. (19) that empty capsids produced in frog kidney tumor cells acquire cores secondarily; however, in the present study, these particles accumulated in the nucleus in unaltered form. There was also no indication that capsids form around previously assembled dense cores, as has been postulated for this virus (12, 42) and herpes simplex virus (33).

Virus particles with double-shelled cores are formed before particles with dense cores in initial stages of infection, are the first particles labeled detectably with  $^3\text{H}$ -thymidine, and do not accumulate appreciably within nuclei or enter the cytoplasm, suggesting that they may be precursors to particles with dense cores. Lunger et al. (19) considered this possibility, on the basis of morphological indications of a condensation of the shell form of core into the dense form. Similar condensation may be involved in core formation in the murine leukemia viruses (8). Alteration of the double-shelled core to the dense form is further indicated by the observation of particles enclosing both shell and dense-core components. However, the mechanism of such a core transformation cannot be ascertained. The outer shell of the double-shelled core may consist of protein; the density of the inner shell may be due to viral DNA incorporated from a nuclear pool during particle coalescence. The shells of immature cores may remain in mature virus particles, in altered form, as inner capsids. Inner capsids have been described for adenoviruses (16) and reoviruses (21), and particles tentatively identified as cores and inner capsids have been observed in

centrifuged preparations of herpes simplex virus (37). Core transformation may also occur in herpes simplex virus, since particles with low-density cores precede the appearance of particles with dense cores (25).

The passage of virus particles into the nuclear envelope, resulting in envelopment by a portion of the inner membrane, is somehow selective for particles with dense cores. Envelopment may result from virus-directed alteration of the inner membrane, which appears to proliferate during infection and becomes markedly thickened wherever contact is made with virus particles. A similar thickening of the inner membrane occurs during envelopment of herpes simplex virus (7, 33). Nuclear sacs may provide an extensive surface area for rapid transport of virus particles into the nuclear envelope. Accumulation of particles in these sacs presumably results from a faster rate of entrance into the nuclear envelope than release into the cytoplasm. Among other herpesviruses, similar nuclear sacs have been reported in cells infected with the herpeslike virus associated with Marek's disease (9) and certain strains of herpes simplex virus (7). Although nuclear envelopment of the frog herpes-type virus appears to be temporary, the nuclear envelope is considered to be a site of permanent envelopment of other herpesviruses (2, 6, 7, 11, 13, 25, 26, 33, 34). In these cases, the entire nuclear envelope is generally thickened and reduplicated, a situation not encountered in infected frog tumor cells. Recently, Nii et al. (25) concluded that envelopment of herpes simplex virus occurs either in the nucleus, in which case particles move through the cytoplasm in vesicles derived from the reduplicated nuclear envelope, or in cytoplasmic vesicles.

Virus particles released into the cytoplasm of infected tumor transplant cells are always coated with a fibrillar material. Herpeslike virus particles in Burkitt lymphoma-derived cell lines and in buffy-coat cells from leukemia patients are often coated with a similar material, although no such coats have been observed on other herpesviruses (5). The possibility that the coat on these herpeslike viruses represents virus-specific antibody (15, 22) suggests that the coat on frog herpes-type virus particles may similarly represent antibody. Although the coat material may be derived directly from sheaths of cytoplasmic filaments composed of similar material (19), this was not evident in the present study, and it is thought that these filaments may represent accumulations of surplus coat material. There is no indication that these solid filaments are similar to the hollow tubules frequently present in the cytoplasm of herpeslike virus-infected cells cultured from Burkitt lymphoma and Marek's

disease and thought to be altered spindle fibers (5, 9, 10).

Final virus envelopment occurs when cytoplasmic particles bud into enlarged vesicles, presumably from the Golgi complex (19); cytoplasmic envelopment of other herpesviruses probably occurs in a similar manner (25). Virus-containing vesicles are occasionally embedded in an electron-dense material which closely resembles the dense layer present in cytoplasmic enveloped particles. This material may be released from lysosomes and hence represent a cell reaction against the virus. Cytoplasmic vesicles containing cytomegalovirus are frequently embedded in a similar dense material thought to represent lysosome material (20, 29).

There is considerable uncertainty as to whether envelopment is essential for herpesvirus infectivity (25, 36, 40, 41). Since the frog herpes-type virus appears to be enveloped at two different stages, it would be of interest to determine the relative infectivity of the nuclear enveloped and cytoplasmic enveloped particles. The presence, in cytoplasmic enveloped forms, of two types of material which may represent cell or host reaction to the virus could affect infectivity.

During herpes-type virus replication in tumor transplant cells, some viral components are apparently produced in significantly greater amounts than are incorporated into complete particles. A 1-hr pulse of  $^3\text{H}$ -thymidine labels virus particles for at least 72 hr, and yet considerable label remains in the nuclear matrix in ethyl alcohol-insoluble form, presumably in DNA. It is unlikely that this residual label represents virus-stimulated cell DNA synthesis, since herpesviruses generally inhibit, rather than stimulate, cellular DNA synthesis (18, 28). It therefore appears that substantially more viral DNA is synthesized than is incorporated into virus particles. Russell et al. (30) found a similar situation in herpes simplex virus-infected cells.

Empty virus capsids are typically produced in large numbers in the frog kidney tumor (12, 19). Fawcett (12) suggested that these particles represent excess production of capsid proteins, and present evidence supports this possibility. The 55-nm particles also accumulate in the nucleus during virus production, frequently forming large aggregates or crystalline arrays. Morphological resemblance to the double-shelled cores of associated virus particles indicates that these particles may represent core structures which have formed spontaneously within the nuclear matrix (38). Similar virus-associated small particles have been described in nuclei infected with herpes simplex (34), herpes simplex hepatitis (27), and pseudorabies (13) viruses, as well as the herpes-type virus associated with Marek's disease (1, 9).

Aberrant virus forms are frequently encountered during virus replication in frog tumor transplant cells. Particles with double-shelled cores are often incomplete, and atypical dense cores are frequently observed in nuclear particles. Similar forms have been described for other herpesviruses (25, 33). Tubular structures observed in advanced infection are considered aberrant virus-related forms and have been described previously (38).

The accumulation in infected tumor transplant cells of surpluses of viral components which remain unincorporated into complete virus particles suggests that virus assembly may occur by chance association of components rather than by an intricate assembly mechanism. The incorporation of core components into capsids may result from the chance entrapment of "soluble" core materials during capsid formation. The greatest production of empty capsids occurs early in virus replication, possibly because intranuclear pools of core materials are so low that chance incorporation into capsids is infrequent. During advanced infection, particles with cores are formed with greater frequency. Core materials may accumulate to a greater extent during advanced infection than capsid proteins, with this imbalance resulting in spontaneous coalescence into corelike particles.

#### ACKNOWLEDGMENTS

I am deeply indebted to Merle Mizell for assistance and advice in all phases of this study.

This investigation was supported by grant E-494 from the American Cancer Society to Merle Mizell, and NIH predoctoral fellowship 5-FI-GM-33,739-02.

#### LITERATURE CITED

1. Ahmed, M., and G. Schidlovsky. 1968. Electron microscopic localization of herpesvirus-type particles in Marek's disease. *J. Virol.* 2:1443-1457.
2. Armstrong, J. A., H. G. Pereira, and C. H. Andrewes. 1961. Observations on the virus of infectious bovine rhinotracheitis, and its affinity with the *Herpesvirus* group. *Virology* 14:276-285.
3. Bernhard, W., H. L. Febvre, and R. Cramer. 1959. Mise en évidence au microscope électronique d'un virus dans des cellules infectées *in vitro* par l'agent du polyome. *Compt. Rend.* 249:483-485.
4. Caspar, D. L. D., and A. Klug. 1962. Physical principles in the construction of regular viruses. *Cold Spring Harbor Symp. Quant. Biol.* 27:1-24.
5. Dalton, A. J., and R. A. Manaker. 1967. The comparison of virus particles associated with Burkitt lymphoma with other herpes-like viruses, p. 59-90. *In* *Carcinogenesis: a broad critique*. Williams & Wilkins Co., Baltimore.
6. Darlington, R. W., and C. James. 1966. Biological and morphological aspects of the growth of equine abortion virus. *J. Bacteriol.* 92:250-257.
7. Darlington, R. W., and L. H. Moss III. 1968. Herpesvirus envelopment. *J. Virol.* 2:48-55.
8. DeHarven, E. 1962. Ultrastructural studies on three different types of mouse leukemia: a review, p. 183-206. *In* A. J. Dalton and F. Haguenuau (ed.), *Tumors induced by viruses: ultrastructural studies*. Academic Press, Inc., New York.
9. Epstein, M. A., B. G. Achong, A. E. Churchill, and P. M.

- Biggs. 1968. Structure and development of the herpes-type virus of Marek's disease. *J. Nat. Cancer Inst.* **41**:805-820.
10. Epstein, M. A., G. Henle, B. G. Achong, and Y. M. Barr. 1965. Morphological and biological studies on a virus in cultured lymphoblasts from Burkitt's lymphoma. *J. Exp. Med.* **121**:761-770.
  11. Falke, D., R. Siegert, and W. Vogell. 1959. Elektronenmikroskopische Befunde zur Frage der Doppelmembranbildung des Herpes-simplex-Virus. *Arch. Gesamte Virusforsch.* **9**:484-496.
  12. Fawcett, D. W. 1956. Electron microscope observations on intracellular virus-like particles associated with the cells of the Lucké renal adenocarcinoma. *J. Biophys. Biochem. Cytol.* **2**:725-742.
  13. Felluga, B. 1963. Electron microscopic observations on pseudorabies virus development in a line of pig kidney cells. *Ann. Scavo* **5**:412-424.
  14. Granboulan, N., P. Tournier, R. Wicker, and W. Bernhard. 1963. An electron microscope study of the development of SV40 virus. *J. Cell Biol.* **17**:423-441.
  15. Henle, W., K. Hummeler, and G. Henle. 1966. Antibody coating and agglutination of virus particles separated from the EB3 line of Burkitt lymphoma cells. *J. Bacteriol.* **92**:269-271.
  16. Horne, R. W. 1962. The comparative structure of adenoviruses. *Ann. N.Y. Acad. Sci.* **101**:475-484.
  17. Jacok, J. 1968. Involvement of the nucleolus in viral synthesis in the cells of primary renal tumors of leopard frogs. *Cancer Res.* **28**:2126-2136.
  18. Kaplan, A. S., and T. Ben-Porat. 1963. The pattern of viral and cellular DNA synthesis in pseudorabies virus-infected cells in the logarithmic phase of growth. *Virology* **19**:205-214.
  19. Lunger, P. D., R. W. Darlington, and A. Granoff. 1965. Cell-virus relationships in the Lucké renal adenocarcinoma: an ultrastructure study. *Ann. N.Y. Acad. Sci.* **126**:289-314.
  20. McGavran, M. H., and M. G. Smith. 1965. Ultrastructural, cytochemical, and microchemical observations on cytomegalovirus (salivary gland virus) infection of human cells in tissue culture. *Exp. Mol. Pathol.* **4**:1-10.
  21. Mayor, H. D., R. M. Jamison, L. E. Jordan, and M. Van Mitchell. 1965. Reoviruses. II. Structure and composition of the virion. *J. Bacteriol.* **89**:1548-1556.
  22. Mayyasi, S. A., G. Schidlovsky, L. M. Bulfone, and F. T. Buscheck. 1967. The coating reaction of the herpes-type virus isolated from malignant tissues with an antibody present in sera. *Cancer Res.* **27**:2020-2024.
  23. Mizell, M., C. W. Stackpole, and S. Halperen. 1968. Herpes-type virus recovery from "virus-free" frog kidney tumors. *Proc. Soc. Exp. Biol. Med.* **127**:808-814.
  24. Morgan, C., H. M. Rose, M. Holden, and E. P. Jones. 1959. Electron microscopic observations on the development of herpes simplex virus. *J. Exp. Med.* **110**:643-656.
  25. Nii, S., C. Morgan, and H. M. Rose. 1968. Electron microscopy of herpes simplex virus. II. Sequence of development. *J. Virol.* **2**:517-536.
  26. Patrizi, G., J. N. Middelkamp, and C. A. Reed. 1967. Reduplication of nuclear membranes in tissue-culture cells infected with guinea-pig cytomegalovirus. *Amer. J. Pathol.* **50**:779-790.
  27. Rabin, E. R., and A. B. Jenson. 1967. Electron microscopic studies of animal viruses with emphasis on in vivo infections. *Progr. Med. Virol.* **9**:392-450.
  28. Roizman, B., and P. R. Roane, Jr. 1964. The multiplication of herpes simplex virus. II. The relationship between protein synthesis and the duplication of viral DNA in infected HEp-2 cells. *Virology* **22**:262-269.
  29. Ruebner, B. H., T. Hirano, R. Slusser, J. Osborn, and D. N. Medearis, Jr. 1966. Cytomegalovirus infection. Viral ultrastructure with particular reference to the relationship of lysosomes to cytoplasmic inclusions. *Amer. J. Pathol.* **48**:971-989.
  30. Russell, W. C., E. Gold, H. M. Keir, H. Omura, D. H. Watson, and P. Wildy. 1964. The growth of herpes simplex virus and its nucleic acid. *Virology* **22**:103-110.
  31. Salpeter, M. M., and L. Bachmann. 1964. Autoradiography with the electron microscope. A procedure for improving resolution, sensitivity, and contrast. *J. Cell Biol.* **22**:469-477.
  32. Séchaud, J., A. Ryter, and E. Kellenberger. 1959. Considérations quantitatives sur des coupes ultramicroscopiques de bactéries infectées par un bactériophage. *J. Biophys. Biochem. Cytol.* **5**:469-477.
  33. Shipkey, F. H., R. A. Erlandson, R. B. Bailey, V. I. Babcock, and C. M. Southam. 1967. Virus biographies. II. Growth of herpes simplex virus in tissue culture. *Exp. Mol. Pathol.* **6**:39-67.
  34. Siegert, R., and D. Falke. 1966. Elektronenmikroskopische Untersuchungen über die Entwicklung des Herpesvirus hominis in Kulturzellen. *Arch. Gesamte Virusforsch.* **19**:230-249.
  35. Siminoff, P., and M. G. Menefee. 1966. Normal and 5-bromodeoxyuridine-inhibited development of herpes simplex virus. An electron microscope study. *Exp. Cell Res.* **44**:241-255.
  36. Smith, K. O. 1964. Relationship between the envelope and the infectivity of herpes simplex virus. *Proc. Soc. Exp. Biol. Med.* **115**:814-816.
  37. Spring, S. B., B. Roizman, and J. Schwartz. 1968. Herpes simplex virus products in productive and abortive infection. II. Electron microscopic and immunological evidence for failure of virus envelopment as a cause of abortive infection. *J. Virol.* **2**:384-392.
  38. Stackpole, C. W., and M. Mizell. 1968. Electron microscopic observations on herpes-type virus-related structures in the frog renal adenocarcinoma. *Virology* **36**:63-72.
  39. Tournier, P., F. Cathala, and W. Bernhard. 1957. Ultrastructure et développement intracellulaire du virus de la varicelle observé au microscope électronique. *Presse Med.* **65**:1229-1234.
  40. Watson, D. H., and P. Wildy. 1963. Some serological properties of herpes virus particles studied with the electron microscope. *Virology* **21**:100-111.
  41. Watson, D. H., P. Wildy, and W. C. Russell. 1964. Quantitative electron microscope studies on the growth of herpes virus using the techniques of negative staining and ultramicrotomy. *Virology* **24**:523-538.
  42. Zambarnard, J., A. E. Vatter, and R. G. McKinnell. 1966. The fine structure of nuclear and cytoplasmic inclusions in primary tumors of mutant leopard frogs. *Cancer Res.* **26**:1688-1700.